

Flow response of magnetic fluid surface by pitching motion[†]

Hyung-Sub Bae, Young-Won Yun and Myeong-Kwan Park*

School of Mechanical Engineering, Pusan National University, Jangjeon-dong, Geumjeong-gu, Busan, 609-735, Korea

(Manuscript Received February 4, 2009; Revised September 27, 2009; Accepted October 12, 2009)

Abstract

This research analyses the dynamic behavior of magnetic fluid that sloshes due to the pitching motion of the container. To analyze the behavior of magnetic fluid, we first analyze the equations that govern magnetic fluid as well as the momentum equation of the sloshing that results from a magnetic field. In each case, we conducted simulation and compared the results from simulation with those from experiments. When sloshing does not occur, the surface of the magnetic fluid rises towards the location of intensity of the magnetic field; in the absence of an additional, external body force, the fluid remains elevated. In case sloshing occurs simultaneously with the application of the magnetic field, the elevation of the surface as a result of the magnetic field is maintained. Further, we can confirm that if the excitation frequency of sloshing is small, the wave motion of the surface is small because the magnetic body force dominates the effect of sloshing. Even if the excitation frequency increases, the wave motion of the fluid surface is smaller than when a magnetic field is not applied. The fluid surface rises in that location where the intensity of the magnetic field is strong. Where the intensity of the magnetic field is weak, the height of the fluid surface is lower than the initial level that obtains in the absence of a magnetic field. Through the study, we can conclude that the sloshing behavior of magnetic fluid is influenced by the magnetic field intensity and distribution.

Keywords: Ferrohydrodynamics; Magnetic body force; Magnetic field; Magnetic fluid; Surface wave

1. Introduction

Usually, fluid in a container is influenced by the motion of the container. Such fluid assumes the form of waves, a phenomenon that is referred as sloshing. Sloshing frequently occurs in fuel tanks of aircraft, ships, etc., and is an important consideration in mechanical design. If sloshing is prolonged or accentuated, the wall of the container is damaged by the body force of the fluid, which in turn, results in unstable behavior of the whole mechanical system. Therefore, we need to clearly understand the sloshing-behavior characteristics of fluids. Published research into the sloshing phenomenon of general fluids theoretically analyzes the characteristics of hydrodynamic behavior through numerical analysis. It also addresses the design of apparatus and fluid-structure interaction, towards the reduction of sloshing. Dongming & Pengzhi, and Ikeda et al. analyzed sloshing using numerical analysis [1, 2]. Abbas et al. investigated the damping of sloshing that arises from the use of baffles in fluid containers [3]. Also, Kim & Cho et al. investigated optimization design technique for sloshing and free surface tracking for nonlinear liquid sloshing [4, 5].

However, sloshing of general fluid is hard to control by it-

self; for reducing sloshing, additional structural elements are required in the fluid container [6-8]. Unlike general fluids, magnetic fluid is a colloidal solution in which separate ferromagnetic particles are distributed evenly in a medium and controllability fluid simultaneously possesses both magnetic and hydrodynamic properties. Magnetic fluid is not settled by gravity, centrifugal forces, magnetic fields, etc. Further, the particles in a magnetic fluid do not cohere. Therefore, if a magnetic field is applied, magnetic fluid is magnetized and the physical and chemical behaviors change so that the fluid can serve as an actuator by itself. Hence, magnetic fluid is advantageous in that its sloshing can be damped without recourse to additional structures, such as baffles, in the fluid container. Magnetic fluid has become an important element in the development of new devices.

Most often, such studies either only address theoretical considerations or only present experimental visualizations [9-11].

In this research, we simultaneously analyze magnetic and hydrodynamic behaviors in the sloshing of magnetic fluid. Through both numerical simulations and experiments, we observe the shape of the surface of magnetic fluid that sloshes in a container.

[†] This paper was recommended for publication in revised form by Associate Editor Gihun Son

*Corresponding author. Tel.: +82 51 510 3089, Fax.: +82 51 514 0685

E-mail address: mkpark1@pusan.ac.kr

2. Ferrohydrodynamics

2.1 Theory

The behavior of magnetic fluid varies with the magnetic field [12-15]. When a magnetic field is not applied, the behavior of magnetic fluid is similar to that of general fluid. However, when a magnetic field is applied, both magnetic and hydrodynamic behaviors need to be simultaneously considered for a magnetic fluid [16-18].

In this research, we analyze first the magnetostatic behavior and then the hydrodynamic behavior of sloshing of magnetic fluid.

2.1.1 Magnetostatic equation

We first conducted magnetostatic analysis because this research concerns the sloshing of magnetic fluid that is under the influence of a magnetic field that arises from a permanent magnet. The magnetostatic behavior can be expressed in terms of Maxwell-Ampere's law and is given by:

$$\nabla \times \vec{H} = \vec{J} \quad (1)$$

Here, $\vec{H}[A/m]$ and $\vec{J}[A/m^2]$ respectively express the magnetic field and current density. Further, because flux has continuity, divergence always becomes '0'. Therefore magnetic flux density $\vec{B}[Wb/m^2]$ is expressed by the Gauss law.

$$\nabla \cdot \vec{B} = 0 \quad (2)$$

To describe the relation between \vec{B} and \vec{H} , we use the constitutive relation:

$$\vec{B} = \mu_0(\vec{H} + \vec{M}(H)) \quad (3)$$

Here, μ_0 is the magnetic permeability in vacuum and $\vec{M}(H)$ is the magnetization due to the magnetic field intensity.

The magnetic vector potential can be also expressed by Eq. (4) and (5) using the identical equation in vector form.

$$\vec{B} = \nabla \times \vec{A} \quad (4)$$

$$\nabla \cdot \vec{A} = 0 \quad (5)$$

Where \vec{A} is the magnetic vector potential, ∇ is the gradient operator.

By substituting in the earlier equations, we arrive at the following vector equation.

$$\nabla \times \vec{A} = \mu_0(\vec{H} + \vec{M}) \quad (6)$$

$$\nabla \times \left(\frac{1}{\mu_0} \nabla \times \vec{A} - \vec{M} \right) = \vec{J} \quad (7)$$

Since this research concerns the sloshing of magnetic fluid

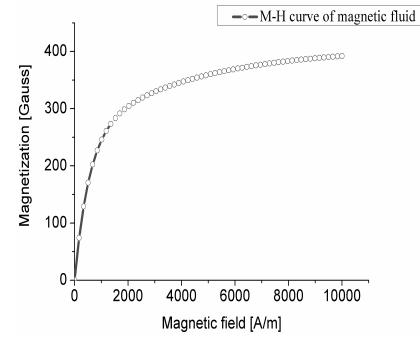


Fig. 1. M-H curve of the magnetic fluid (W-40).

in two-dimensions, the current density $\vec{J} = 0$. Eq. (7) can be rewritten as:

$$\nabla \times \left(\frac{1}{\mu_0} \nabla \times \vec{A} - \vec{M} \right) = 0 \quad (8)$$

Fig. 1 shows the variation of the magnetization with the magnetic field intensity of the magnetic fluid (W-40, Taiho industry, Japan) that is used in this research.

As the figure shows, as the magnetic field intensity continuously increases, the magnetization of magnetic fluid asymptotically approaches a specific value known as the saturation magnetization.

Since the saturation magnetization of magnetic fluid appeared from $3600[A/m]$ ($450[Gauss]$), we defined the magnetic field intensity that applied maximum $500[Gauss]$ low.

2.1.2 Governing equation of magnetic fluid sloshing

When magnetic field is applied, both electromagnetic and hydrodynamic properties of magnetic fluid must be considered.

Therefore, the flow that is induced by sloshing must satisfy the continuity and momentum equations that are similar to the case of general fluids. The equations are given below.

$$\frac{\partial u}{\partial x} + \frac{\partial v}{\partial y} = 0 \quad (9)$$

$$\rho \frac{\partial \vec{u}}{\partial t} - \nabla \cdot \eta(\nabla \vec{u} + (\nabla \vec{u})^T) + \rho(\vec{u} \cdot \nabla) \vec{u} + \nabla p_c = \vec{F}_m + \vec{F}_v \quad (10)$$

Here, ρ is the density of the magnetic fluid, $\vec{u} = (u, v)$ is the velocity, η is the dynamic viscosity, $p_c = p_f + p_m$ is the composite pressure with the fluid pressure p_f and the fluid-magnetic pressure p_m when the small applied magnetic field;

$$\begin{aligned} p_m &\equiv \mu_0 \int_0^H M dH = \mu_0 \vec{M} H = \mu_0 \left(\frac{1}{H} \int_0^H M dH \right) H \\ &= \frac{\mu_0}{2} M H \end{aligned} \quad (11)$$

Eq. (11) expresses fluid pressure difference that happens inner and external by a magnetic field and these are relevant to the surface elevation of magnetic fluid.

Therefore, we can express the magnetic body force $\vec{F}_m = \mu_0(\vec{M} \cdot \nabla)\vec{H}$ in Cartesian coordinates by using the magnetic vector potential \vec{A} that is given by:

$$(F_m)_x = \mu_0 \left(M_x \frac{\partial H_x}{\partial x} + M_y \frac{\partial H_x}{\partial y} \right) = \mu_0 \left(M_x \frac{\partial}{\partial x} \frac{1}{\mu_0 \mu_r} \frac{\partial A_z}{\partial y} - M_y \frac{\partial}{\partial y} \frac{1}{\mu_0 \mu_r} \frac{\partial A_z}{\partial x} \right) \quad (12)$$

$$(F_m)_y = \mu_0 \left(M_x \frac{\partial H_y}{\partial x} + M_y \frac{\partial H_y}{\partial y} \right) = \mu_0 \left(-M_x \frac{\partial}{\partial x} \frac{1}{\mu_0 \mu_r} \frac{\partial A_z}{\partial x} + M_y \frac{\partial}{\partial y} \frac{1}{\mu_0 \mu_r} \frac{\partial A_z}{\partial x} \right) \quad (13)$$

\vec{F}_v is the body force that is imposed on the fluid by the motion of the container, it can be expressed in Cartesian coordinates in the following manner.

$$(F_v)_x = \rho g \sin(\phi_{\max} \sin(2\pi ft)) \quad (14)$$

$$(F_v)_y = -\rho g \cos(\phi_{\max} \sin(2\pi ft)) \quad (15)$$

The magnetization, \vec{M} can be expressed in cartesian coordinates by using the Langevin function in the above equation.

$$\lim_{\alpha \gg 1} M_x = M_s \left(1 - \frac{1}{\alpha}\right) = M_s \left\{1 - \frac{6kT}{\pi \mu_0 \phi M_d H_x d^3}\right\} \quad (16)$$

$$\lim_{\alpha \gg 1} M_y = M_s \left(1 - \frac{1}{\alpha}\right) = M_s \left\{1 - \frac{6kT}{\pi \mu_0 \phi M_d H_y d^3}\right\} \quad (17)$$

In addition, each variable that appears in Eq. (16) and (17) is listed in Table 1.

But magnetic field is small that was applied to the magnetic fluid in this system.

So the Langevin function is approximately linear, hence the magnetization is proportional to the effective field strength.

Table 1. Parameters of the Langevin equation.

$M_s = \phi M_d$	Magnetic saturation of magnetic fluid [A/m]
M_d	Particle magnetization in [A/m]
ϕ	Volume fraction of magnetic particles
α	$\frac{\mu_0 M_d V H}{KT}$, energy ratio
V	Magnetic volume of spherical magnetic fluid
d	Nano particles of diameter, 7 [nm]
T	Temperature in Kelvin, 298 [K]

$$\vec{M} = \chi_{mf} \vec{H} \quad (18)$$

Here, χ_{mf} is the magnetic susceptibility of magnetic fluid.

By incorporating the above numerical formulae, we can express Eq. (10) in terms of Cartesian coordinates.

$$\rho \frac{\partial u}{\partial t} = -\frac{\partial p_c}{\partial x} + \eta \left(\frac{\partial^2 u}{\partial x^2} + \frac{\partial^2 u}{\partial y^2} \right) - \rho \left(u \frac{\partial u}{\partial x} + v \frac{\partial u}{\partial y} \right) + \mu_0 \left(M_x \frac{\partial}{\partial x} \frac{1}{\mu_0 \mu_r} \frac{\partial A_z}{\partial y} - M_y \frac{\partial}{\partial y} \frac{1}{\mu_0 \mu_r} \frac{\partial A_z}{\partial x} \right) + \rho g \sin(\phi_{\max} \sin(2\pi ft)) \quad (19)$$

$$\rho \frac{\partial v}{\partial t} = -\frac{\partial p_c}{\partial y} + \eta \left(\frac{\partial^2 v}{\partial x^2} + \frac{\partial^2 v}{\partial y^2} \right) - \rho \left(u \frac{\partial v}{\partial x} + v \frac{\partial v}{\partial y} \right) + \mu_0 \left(-M_x \frac{\partial}{\partial x} \frac{1}{\mu_0 \mu_r} \frac{\partial A_z}{\partial x} + M_y \frac{\partial}{\partial y} \frac{1}{\mu_0 \mu_r} \frac{\partial A_z}{\partial x} \right) - \rho g \cos(\phi_{\max} \sin(2\pi ft)) \quad (20)$$

Eq. (19) and (20) express the sloshing of magnetic fluid that also includes the impact of the magnetic body force. The left-hand-sides of Eq. (19) and (20) refer to the distribution of the rate of change of velocity of the fluid. The right-hand-sides of Eq. (19) and (20) are expressed in terms of the pressure, viscosity, magnetic body force, and body force, including gravity.

We can know that Eq. (19) and (20) can be recast in a manner that corresponds to *Ferrohydrodynamics*, wherein the behavior of magnetic fluid is expressed and the body forces, including gravity, are incorporated.

3. Simulation

3.1 Magnetic field analysis

In the context of the sloshing of magnetic fluid, regardless of whether a magnetic field is applied, the electromagnetic property of the fluid must be considered.

In this study, the magnetic field is created by a permanent

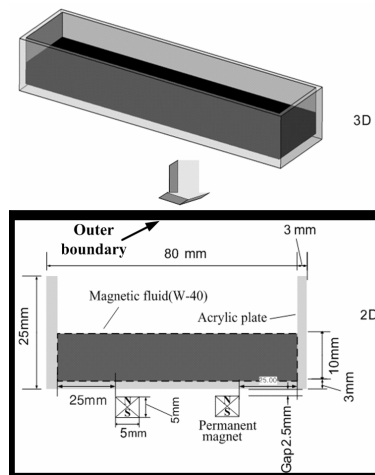


Fig. 2. Model for analyzing sloshing of magnetic fluid.

magnet. Therefore, it was important to conduct magnetostatic analysis in two dimensions. In this research, simulation was achieved by the COMSOL multiphysics.

COMSOL Multiphysics is the interactive software for modelling and solving scientific and engineering problems based on partial differential equations (PDEs). This environment runs finite element analysis together with adaptive meshing and error control using a variety of numerical solvers. COMSOL Multiphysics converts all application mode and PDE mode equation formulations and systems to the weak form before solving them with the finite element method.

Fig. 2 depicts a model that is used to analyze the sloshing of magnetic fluid.

The permanent magnet that is used in this research is neodymium (Nd) series. It is of size $18\text{mm} \times 5\text{mm} \times 5\text{mm}$. The surface magnetic flux density and the relative magnetic permeability are each about 3000 [Gauss], 1.05.

In Fig. 2, the gap between the magnet and the fluid container is set to 2.5mm, which is within the range in which the spike phenomenon does not occur at the surface of the magnetic fluid. Further, we defined the distance between the magnets that were kept at 40mm lest the behavior of magnetic fluid is affected when the container is stationary.

First, we get the magnetic vector potential \vec{A} using the COMSOL multiphysics. And then magnetic flux density \vec{B} was obtained from the relation of \vec{B} and \vec{A} in Eq. (4). Also, \vec{H} was obtained from the relation of $\vec{B} = \mu_0\mu_r\vec{H}$. In this study, magnetic field from the permanent magnet is about 3000 [Gauss] but magnetic field that was applied actually to the magnetic fluid was small.

The boundary conditions in the magnetostatic analysis for the magnetic fluid system can be expressed respectively as follows;

$$\vec{n} \cdot (\vec{B}_{\text{magnetic fluid}} - \vec{B}_{\text{air}}) = 0 \tag{21}$$

$$\vec{n} \times (\vec{H}_{\text{air}} - \vec{H}_{\text{magnetic fluid}}) = 0 \tag{22}$$

Where, first equation states that the component of \vec{B} normal to the interface is continuous. And second equation states that the tangential component of magnetic field is continuous. And magnetic insulation condition was applied to the outer boundary in Fig. 2. Also, initial condition of magnetic vector potential \vec{A} for calculating the magnetic field, magnetic flux density and magnetization was zero, $A_z = 0$.

Fig. 3 and 4 respectively show the distributions of the magnetic flux density and magnetic field intensity at increments of 2.5mm from the surface of the magnet.

The magnetic flux density is confirmed to be the largest (3000 Gauss) at the surface of the magnet.

As Fig. 3 illustrates, it decreases as the distance from the magnet's surface increases.

Fig. 4 shows that when the distance from the magnet's surface is at most 2.5mm, the magnetic field intensity is considerably greater at the corner of the magnet than at the center.

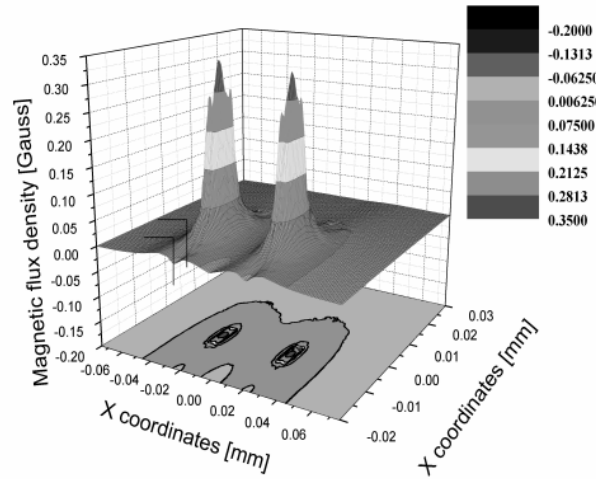


Fig. 3. 3-D distribution of the magnetic flux density.

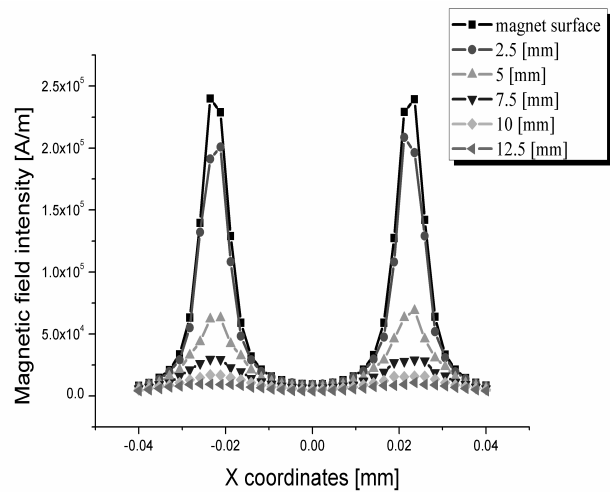


Fig. 4. Distribution of the magnetic field intensity.

However, when the distance exceeds 5mm, the magnetic field intensity at the corner rapidly decreases.

Further, we can know that even if the magnetic field intensity of the permanent magnet is 3000 [Gauss], only about 300-600 [Gauss] actually acts upon the fluid inside the container, in light of the thickness of the container and the gap between the magnet and the container.

3.2 Analysis of the static behavior of magnetic fluid

As with Eq. (10), the governing equation for magnetic fluid can be obtained by incorporating the magnetic body force in a Navier-Stoke's equation.

In this research, interactions between fluid particles are excluded from consideration. We first analyze the behavior of magnetic fluid that is under the influence of a magnetic body force before analyzing the impact of sloshing on the fluid.

Therefore, the equations that govern the sloshing of magnetic fluid are derived by eliminating \vec{F}_v from Eq. (19) and (20), as follows:

$$\rho \frac{\partial u}{\partial t} = -\frac{\partial p_c}{\partial x} - \eta \left(\frac{\partial^2 u}{\partial x^2} + \frac{\partial^2 v}{\partial y^2} \right) - \rho \left(u \frac{\partial u}{\partial x} + v \frac{\partial u}{\partial y} \right) + \mu_0 \left(M_x \frac{\partial}{\partial x} \frac{1}{\mu_0 \mu_r} \frac{\partial A_z}{\partial y} - M_y \frac{\partial}{\partial y} \frac{1}{\mu_0 \mu_r} \frac{\partial A_z}{\partial x} \right) \tag{23}$$

$$\rho \frac{\partial v}{\partial t} = -\frac{\partial p_c}{\partial y} - \eta \left(\frac{\partial^2 u}{\partial x^2} + \frac{\partial^2 v}{\partial y^2} \right) - \rho \left(u \frac{\partial v}{\partial x} + v \frac{\partial v}{\partial y} \right) + \mu_0 \left(-M_x \frac{\partial}{\partial x} \frac{1}{\mu_0 \mu_r} \frac{\partial A_z}{\partial x} + M_y \frac{\partial}{\partial y} \frac{1}{\mu_0 \mu_r} \frac{\partial A_z}{\partial x} \right) \tag{24}$$

And, there are two types of boundaries in the model domain. Three solid walls are modeled with no-slip conditions, and one free boundary (the top boundary). The boundary condition for the sloshing of magnetic fluid is given by

$$\vec{u} = 0 \tag{25}$$

The fluid is free to move on the top boundary. The stress in the surrounding environment is neglected. Therefore the stress continuity condition on the free boundary reads

$$(-p\vec{I} + \eta(\nabla\vec{u} + (\nabla\vec{u})^T)) \cdot \vec{n} = -p_0\vec{n} \tag{26}$$

Where p_0 is the surrounding (constant) pressure and η the viscosity in the fluid. Without loss of generality, $p_0 = 0$ for this model.

Eq. (25) and (26) indicate a no-slip boundary condition for the three walls and a free boundary condition for the fluid surface. Further, $\vec{u} = (u, v)$ is the fluid velocity, p is the pressure, I is the unit diagonal matrix, and p_0 refers to the surrounding pressure.

By above equations, magnetic field and magnetization is calculated by magnetic vector potential. So, outer boundary condition of magnetic vector potential in Fig. 2 was set by magnetic insulation. This implies that the magnetic vector potential is zero at the outer boundary, corresponding to a zero magnetic flux and all initial condition of magnetic vector potential is zero.

The density and viscosity of the magnetic fluid that is used in this research are respectively $1350 \times 10^3 [kg/m^3]$ and $3.99 \times 10^{-2} [kg/m \cdot s]$. The gravity, g , is $9.8 [m/s^2]$ and volume of magnetic fluid is $25cc$.

Fig. 5 and 6 show the results of two and three-dimensional analyses of the behavior of magnetic fluid when a magnetic body force is applied and the surface of the magnetic fluid rise by about $2.7 \pm 0.2mm$. In the absence of an additional external body force, the fluid surface remains elevated.

The surface elevation of the magnetic fluid is highest where the magnetic field intensity is strong. On the other hand, where the magnetic field intensity is weak, the elevation of the surface is lower than when a magnetic field is not applied.

This phenomenon can be explained as follows. When a magnetic field is applied, a pressure difference arises inside the magnetic fluid. Since the pressure difference generates a

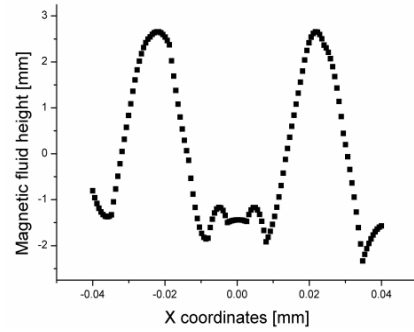


Fig. 5. Surface height of the magnetic fluid.

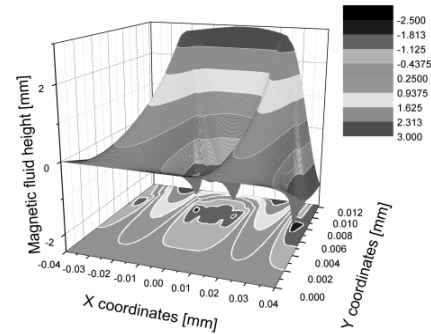


Fig. 6. 3-D surface height of the magnetic fluid.

flow of magnetic fluid and surface elevation occurs, fluid moves to where the magnetic field is strong.

Therefore, if the magnetic field intensity rises (but is under the saturation magnetization), the magnetic body force increases and the surface of the magnetic fluid is elevated more.

However, if a magnetic field intensity that is larger than the saturation magnetization is applied, or if the volume of fluid is small in relation to the applied magnetic field, the spike phenomenon can occur in the resulting region of instability that is studied by other researchers [19].

Through these results, we can estimate that the flow of magnetic fluid is related to magnetic field intensity and distribution under the spike phenomenon is not appeared.

3.3 Analysis of sloshing of magnetic fluid

The sloshing of magnetic fluid can be analyzed by adding Eq. (14) and (15) that expresses the dynamic behavior of fluid in the container to Eq. (23) and (24).

For analyzing the sloshing of magnetic fluid, the pitching motion of the container is integrated with the results from the analysis of the static behavior of magnetic fluid that had been discussed in the preceding section. And for calculating the free surface of magnetic fluid used the ALE (Arbitrary Lagrangian-Eulerian) method that is offered from the COMSOL multiphysics. In order to the motion of the fluid with the moving mesh, it is necessary to couple the mesh motion to the fluid motion normal to the surface. It turns out that for this type of free surface motion, it is important to not couple the mesh motion to the fluid motion in the tangential direction.

So, the boundary condition for the mesh equations on the free surface is therefore

$$(x_t, y_t)^T \cdot \vec{n} = \vec{u} \cdot \vec{n} \quad (27)$$

where \vec{n} is the boundary normal and $(x_t, y_t)^T$ the velocity of mesh.

Therefore, free surface of magnetic fluid is calculated by pressure that interacts on the fluid surface using the Eq. (26).

The pitching angle and excitation frequency of the container are respectively set to $2^\circ\text{--}4^\circ$ and $0.5\text{Hz} \sim 3\text{Hz}$.

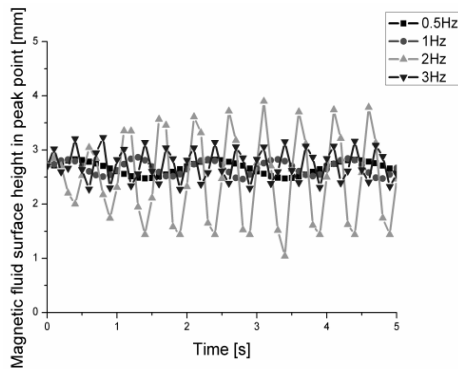


Fig. 7. The height of the surface of the magnetic fluid at the center (pitching angle of 2°).

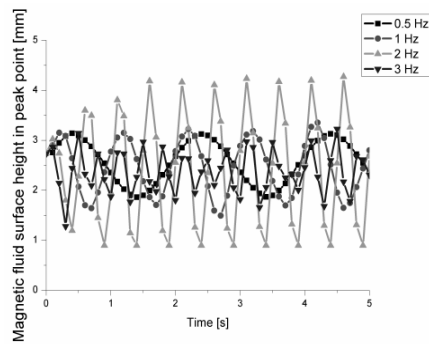


Fig. 8. The height of the surface of the magnetic fluid at the center (pitching angle of 3°).

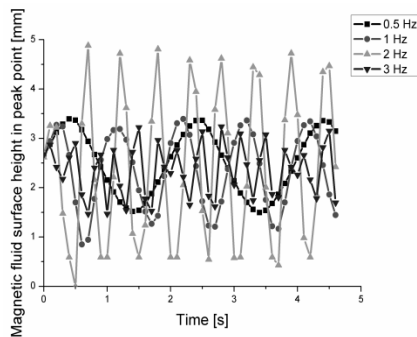


Fig. 9. The height of the surface of the magnetic fluid at the center (pitching angle of 4°).

First, we analyze the behavior of the surface of the magnetic fluid at two locations: the location of the permanent magnet and the edge of the container.

Fig. 7-9 demonstrates the change in the height of the free surface of the magnetic fluid over time, for various angles of pitching and excitation frequencies.

Unlike general fluids, magnetic fluids are influenced by magnetic fields; the magnetic fluid retains an initial elevation of about $2.7 \pm 0.2\text{mm}$ before the excitation frequency is applied and then sloshing phenomenon was occurred.

The initial elevation, which arises due to the magnetic field, is retained even as the excitation frequency increases. Unlike general fluids, the sloshing of the magnetic fluid is controlled by the magnetic field.

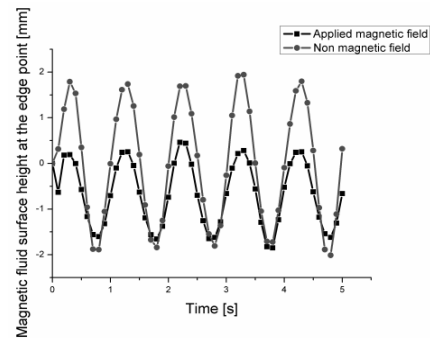


Fig. 10. Comparison between the presence and absence of a magnetic field (pitching angle of 2° and excitation frequency of 1Hz).

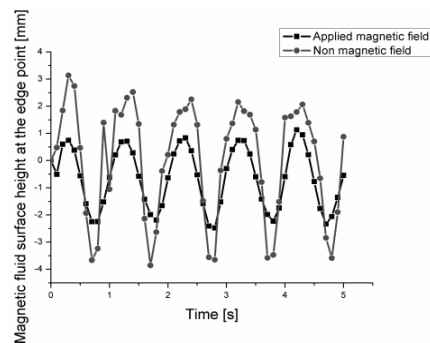


Fig. 11. Comparison between the presence and absence of a magnetic field (pitching angle of 3° and excitation frequency of 1Hz).

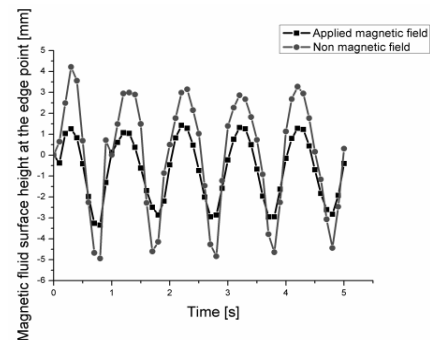


Fig. 12. Comparison between the presence and absence of a magnetic field (pitching angle of 4° and excitation frequency of 1Hz).

The change in height of the surface of the magnetic fluid initially increases with the excitation frequency during the uniform angle of pitching. Owing to resonance, the sloshing of magnetic fluid is maximized at 2Hz and decreases once the excitation frequency lies outside the region of resonance.

Fig. 10-12 shows the behavior of the surface at the edge of the container, under an excitation frequency of 1Hz and each of three angles of pitching. The figures clarify the impact of the magnetic field on the sloshing behavior of magnetic fluid.

In the absence of a magnetic field, the sloshing behavior, when the container is pitched, of a magnetic fluid is similar to that of a general fluid. And sloshing is accentuated than in the absence of a magnetic field.

In the presence of a magnetic field, fluid flows to the location where the magnetic field intensity is strong. Where the magnetic field intensity is weak, the surface of the fluid becomes below the initial height that magnetic field is not applied.

Even if the intensity of the magnetic field is weak, magnetic fluid seeks to retain its form during pitching because it possesses the magnetization property.

4. Experiment

Fig. 13 depicts a schematic diagram of the experiment. Fig. 14 is a three-dimensional schematic diagram of the sloshing device that shows: a step motor for pitching the container; the fluid container; and a portion of the permanent magnet. The container is filled with magnetic fluid and the permanent magnet is situated below the container, 2.5mm from the bottom.

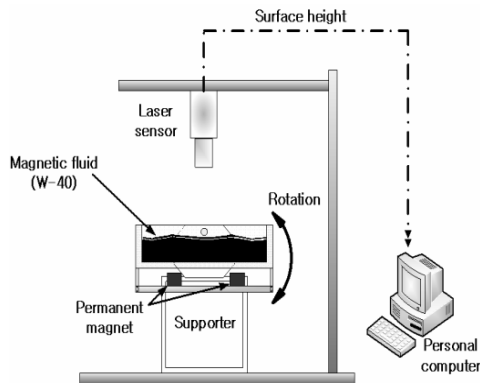


Fig. 13. Schematic diagram of the experiment.

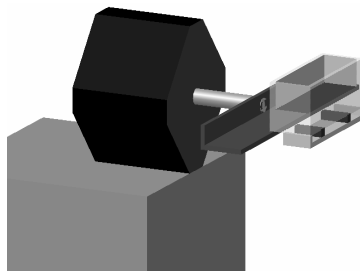


Fig. 14. Three-dimensional schematic diagram of the sloshing device.

The step motor is controlled for applying various angles of pitching and excitation frequencies to simulate cyclic sloshing of the container.

Since the magnetic fluid that is used in this research is opaque and black, and can stick to the outer wall of the device during experiments, it is difficult to measure sloshing behavior through visualization or sensors. In particular, because the laser pointer is absorbed in the magnetic fluid, measurement using the laser sensors becomes ineffective.

To solve this problem in the present study for the measurement of surface behavior, aluminum powder (200mesh, Junsei chemical) is spread on the magnetic fluid to form a thin film on the surface.

Therefore, we first conducted a sloshing experiment with

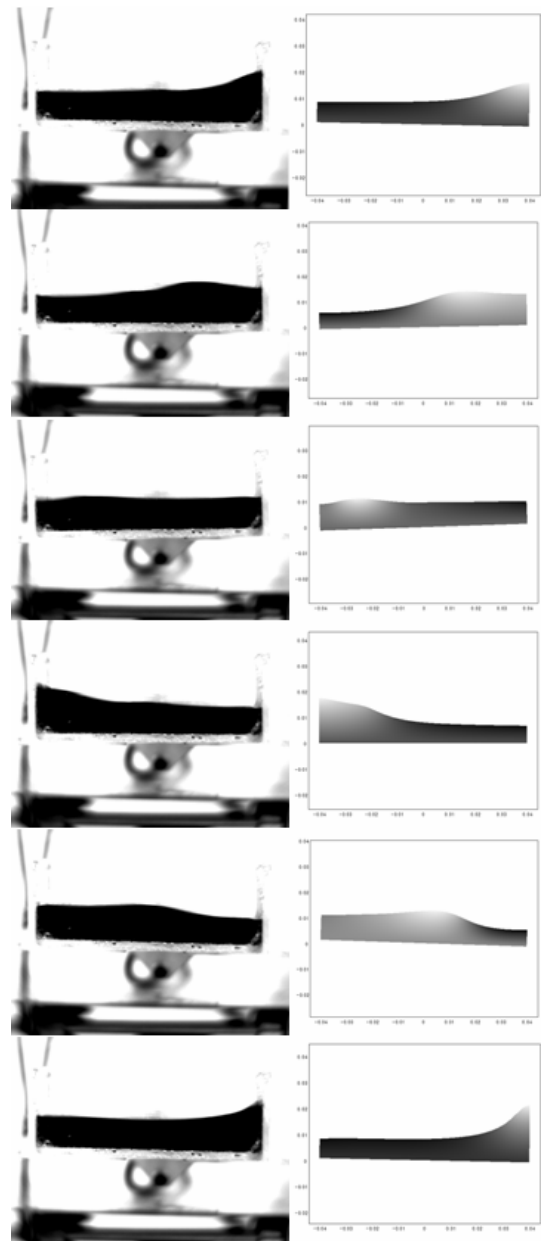


Fig. 15. Simulation and experiment of the sloshing of water.

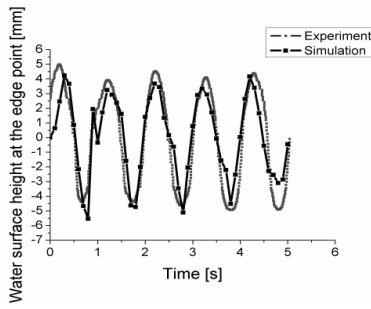


Fig. 16. Simulation and experiment with the sloshing of water (angle of pitching 2°, excitation frequency 1Hz).

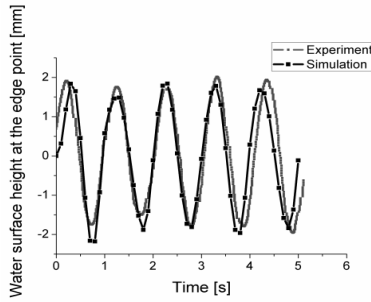


Fig. 17. Simulation and experiment with the sloshing of water (angle of pitching 3°, excitation frequency 1Hz).

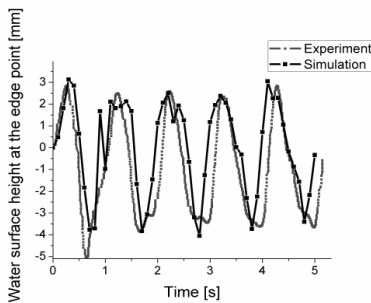


Fig. 18. Simulation and experiment with the sloshing of water (angle of pitching 4°, excitation frequency 1Hz).

Fig. 16-18 compares the simulation and experimental results for various angles of pitching and an excitation frequency of 1Hz. While some phase difference exists, the top and bottom displacements of the fluid surface are almost in agreement across both the simulation and the experimental results.

Given that the amount of aluminum powder is very little, we can confirm that the powder does not affect the sloshing behavior of the fluid.

For various angles of pitching and excitation frequencies, Fig. 19 compares the simulation and experimental results of the behavior of the fluid surface that occurs at the side-wall of the container due to the sloshing of magnetic fluid. In case the angles of pitching and excitation frequencies are small, the simulation and experimental results agree almost perfectly.

Fig. 16-18 suggests that when the angles of pitching and excitation frequencies are same, the amplitude of fluctuation

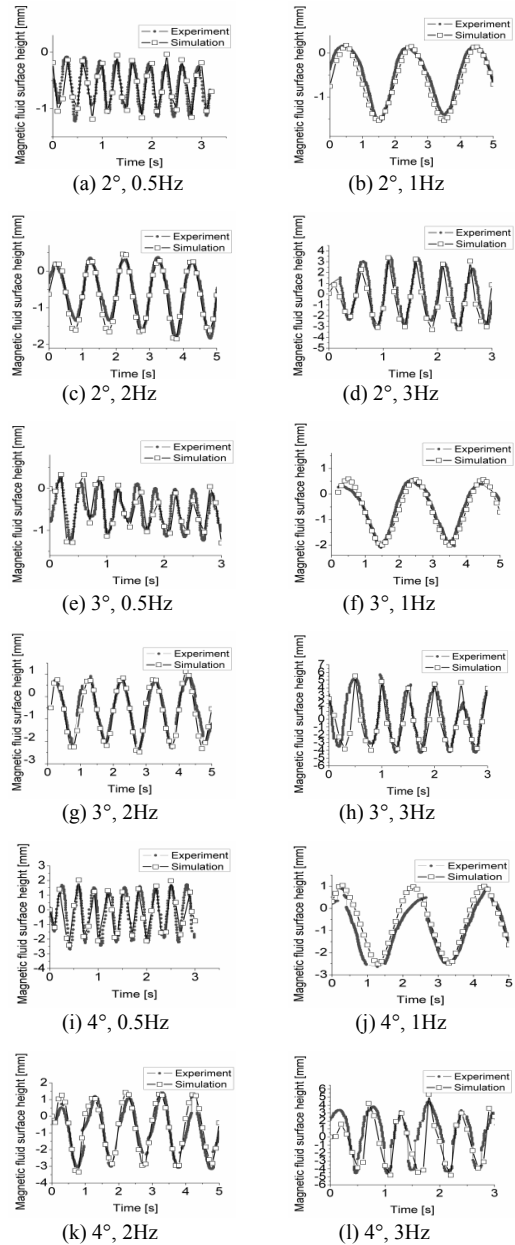


Fig. 19. Simulation and experiment results of the magnetic fluid sloshing at the edge point.

in the height of the fluid surface, as a result of sloshing, is greater for water than for magnetic fluid.

Since the magnetic fluid is magnetized, it will cohere towards the locations where the magnetic field intensity is strong.

When both the angles of pitching and excitation frequencies were small, the sloshing of the magnetic fluid displayed stable behavior. This was also true when the angles of pitching were large but excitation frequencies were small.

In addition, the amplitude of fluctuation of the fluid surface is relatively very high at 2Hz, owing to resonance, and decreases at a frequency of 3Hz; this experimental findings accords well with the result from simulation.

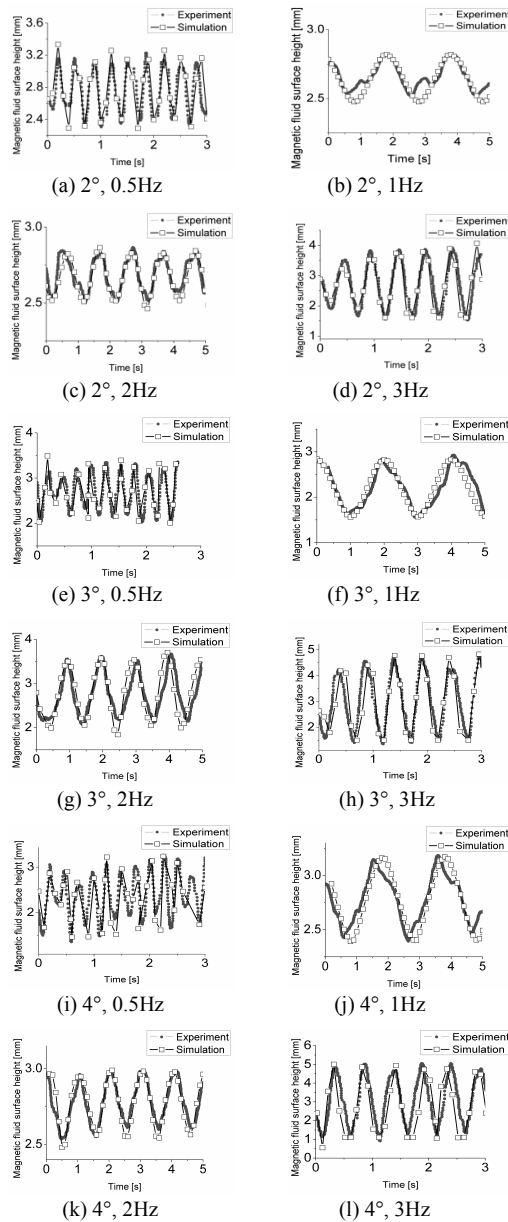


Fig. 20. Simulation and experiment results of the magnetic fluid sloshing at the center point.

Fig. 20 compares the simulation and experimental results of the sloshing of magnetic fluid at the center of the permanent magnet, where the height of the fluid surface peaks. The results from simulation and the experiment are almost similar. In the case of low excitation frequencies, the wave motion of the surface is small (about 1mm). This reason is that magnetization occurs more intensely in the vicinity of the magnet and the cohesive force of fluid is growing.

In other words, when the fluid container is subject to a low excitation frequency, the magnetic body forces are stronger than the body forces that arise from the movement of the container. In turn, this curtails the dispersion of fluid.

However, if the angles of pitching and excitation frequencies are simultaneously increased, the external body force that

arises from sloshing exceeds the magnetic body force. Then, the behavior of the fluid surface is irregular.

5. Conclusions

We have analyzed the relationship between the magnetic field distribution and the hydrostatic properties of magnetic fluid. We have also confirmed comparative analysis of the results from simulation and experiments on the sloshing phenomenon.

A magnetic field from a permanent magnet acts upon the magnetic fluid in the manner of an external, magnetic body force. As a result of this force, the surface elevates. Further, in the presence of the magnetic field, for each angle of pitching by which the container is sloshed, the surface of the fluid that is located close to the magnet remains elevated at a initial level under low excitation frequencies. In other words, the change in the surface elevation is small.

The magnitude of the surface wave near the container wall is smaller for a magnetic fluid, under the influence of a magnetic field, compared to that for water. Since magnetic fluid flows towards the location of strong intensity of the magnetic field, the surface height of fluid that is sloshing can become lower than the initial surface height that obtains in the absence of a magnetic field.

This research reveals that the sloshing of magnetic fluid can be controlled by the volume of fluid and the magnetic field intensity. We may control sloshing behavior in a more stable manner if establish magnet or electromagnet and escape the interference of magnetic field. Therefore, this research may act an important role in the context of basic research that is necessary for developing a new type of actuators that uses magnetic fluid.

References

- [1] D. Liu and P. Lin, A numerical study of three-dimensional liquid sloshing in tanks, *J Comput. Phys.*, 227 (8) (2008) 3921-3939.
- [2] T. Ikeda and R. A. Ibrahim, Nonlinear random responses of a structure parametrically coupled with liquid sloshing in a cylindrical tank, *J Sound. Vib. Inter.* 284 (1-2) (2005) 75-102.
- [3] M. Abbas and Z. Mansour, Sloshing damping in cylindrical liquid storage tanks with baffles, *J Sound. Vib. Inter.* 311 (1-2) (2008) 372-385.
- [4] H. S. Kim and Y. S. Lee, Optimization design technique for reduction of sloshing by evolutionary methods, *Journal of Mechanical Science and Technology.* 22 (2008) 25-33.
- [5] J. R. Cho and H. W. Lee, Free Surface Tracking for the Accurate Time Response Analysis of Nonlinear Liquid Sloshing, *Journal of Mechanical Science and Technology.* 19 (7) (2005) 1517-1525.
- [6] S. Kamiyama, K. Ueno and Y. Yokota, Numerical analysis of unsteady gas-liquid two-phase flow of magnetic fluids, *J*

- Magn. Magn. Mater. 201 (1-3) (1999) 271-275.
- [7] V. G. Bashtovoy, O. A. Lavrova, V. K. Polevikov and L. Tobiska, Computer modeling of the instability of a horizontal magnetic-fluids layer in a uniform magnetic field, *J Magn. Magn. Mater.* 252 (2002) 299-301.
- [8] R. Badescu, D. Condurach and M. Ivanoiu, Ferrofluid with Modified Stabilisant, *J Magn. Magn. Mater.* 202 (1) (1999) 197-202.
- [9] M. I. Shliomis and B. L. Smorodin, Convective Instability of Magnetized Ferrofluids, *J Magn. Magn. Mater.* (252) (2002) 197-202.
- [10] K. Butter, A. P. Philipse and G. J. Vroege, Synthesis and properties of iron ferrofluids, *J Magn. Magn. Mater.* 252 (2002) 1-3.
- [11] M. Rasa and A. P. Philipse, Scanning probe microscopy on magnetic colloidal particles, *J Magn. Magn. Mater.* 252 (2002) 101-103.
- [12] R. Rosensweig, *Ferrohydrodynamics*, Cambridge: Cambridge University Press, 1985.
- [13] R. Yamane, S. Tomita, J. Mai, M. K. Park and S. Oshima, Oscillation of a diamagnetic liquid bubble suspended by magnetic force, *J Magn. Magn. Mater.* 252 (2002) 268-270.
- [14] R. Yamane, S. Ryuichiro, S. Oshima and M. K. Park, Magnetically suspended virtual divergent channel, *J Magn. Magn. Mater.* 289 (2005) 389-391.
- [15] S. Kamiyama, K. Koike and Z. S. Wang, Rheological properties of magnetic fluids with the formation of clusters: analysis of simple shear flow in a strong magnetic field, *J Collo. and Inter. Sci.* 127 (1) (1989) 173-188.
- [16] C. Rindaldi, F. Gutman, X. He, A. D. Rosenthal and M. Zahn, Torque Measurement on Ferrofluid Cylinders in Rotating Magnetic Fields, *J Magn. Magn. Mater.* 289 (2005) 307-310.
- [17] A. Zeuner, R. Richter and I. Rehberg, Weak Periodic Excitation of a Magnetic Fluid Capillary Flow, *J Magn. Magn. Mater.* 201 (1-3) (1999) 321-323.
- [18] M. Kroell, M. Prodoehl, G. Zimmermann, S. Pop and S. Odenbach, A. Hartwig, Magnetic and Rheological Characterization of Novel Ferrofluids, *J Magn. Magn. Mater.* 289 (2005) 21-24.

- [19] S. Sudo, I. Kazutaka and I. Toshiaki, Dynamics of Magnetic Fluid-Permanent Magnet System Subjected to Vertical Vibration, *J Intel. Mater. Sys. Struc.* 13 (2002) 539.



Hyung-Sub Bae received the M.S. degrees in Mechanical Engineering from Pusan National University, Korea, in 2004. His research interests are in hydraulic and smart fluid control such as magnetic fluid and MR fluid.



Young-Won Yun was born in Busan, Korea, in 1973. He received his B.S. in Mechanical Engineering from Donga University, Busan, Korea, in 2000. He also received his M.S. in Mechanical Engineering from Pusan National University, Busan, Korea, in 2003. He is currently working toward his Ph. D at

Pusan National University. His current research interests are Electro-hydraulic systems and a robust controller.



Myeong-Kwan Park received the M.S. and Ph.D. degrees from Tokyo Institute of Technology, Tokyo, Japan, in 1988 and 1991, respectively, in mechanical engineering. From 1991 to 1992, he served as a Research Associate in Department Mechanical Engineering, Tokyo Institute of Technology. He is currently

a full professor with Department of Mechanical Engineering and a Researcher in the Research Institute of Mechanical Technology at Pusan National University. His research interests are in hydraulic and smart fluid such as magnetic fluid, ER fluid and MR fluid.